



Thermodynamic and Nonlinear Kinetic Modelling Behaviours of Lead (II) Adsorption on Functionalized and Carbonized Groundnut Husk

Ikemefuna Usifoh, M.U. Obidiegwu and C. R. Odinigwe

Polymer and Textile Engineering, Federal University of Technology Owerri, Owerri, Imo, Nigeria

ABSTRACT

This work was based on the removal of Lead from waste water using Carbonized and Functionalized lignocellulose Groundnut husk. Several modification techniques were used to produce three adsorbents GS-HCLC (Groundnut shell modified with HCl and ZnCl² and then carbonized at 400 °C), GS-KOHC (Groundnut shell modified with KOH and then carbonized at 400 °C) and GS-TPP (Groundnut shell functionalized using Tripolyphosphate) for the adsorption of Pb²⁺ ions from aqueous solution. Proximate, Ultimate and Elemental analysis was carried out on the adsorbents. Excel solver was used for non-linear kinetic models; Intra particle diffusion model, Pseudo First order and Pseudo Second order and also thermodynamics of the adsorption process was studied. Pseudo Kinetic second order model was best used to describe the kinetics of adsorption for GS-HCLC and GS-KOHC while Intraparticle diffusion best describes the kinetics of adsorption for GS-TPP. The thermodynamics of adsorption was found to be feasible and spontaneous except during the adsorption by the GS-TPP adsorbent while the enthalpy was positive across all adsorbents during adsorption.

Key words: Thermodynamics, Kinetics, lead, adsorption, Groundnut husk

1. INTRODUCTION

Water is one of the most essential items needed in the ecological systems for the maintenance and sustainability of the lives of plants and animals. Waste water or contaminated water poses great challenge to ecological systems since time immemorial because water is one of the fundamental elements of living. Water can be contaminated through various actions either naturally by unprecedented activities (such as earthquakes, volcanoes, naturally stored heavy metal deposits, natural flow effluent into water bodies, acidic rainfall, etc.) or by man's action in the cause of science technological advancement or generally plain ignorance [1]. Heavy metals when consumed in quantities above the normal stipulated amount have been known to be toxic leading to disabilities, cancer and ultimately death to all forms of life [2]. The major source of these heavy metal contamination is from industrial sources such as textile dyes and mills, semi-conductor manufacturers, printed board manufacturers, metal finishing and plating industry and also paint industries. Other minor sources may be from runoffs and landfills. The type of water contamination differs likewise the different methodology of water treatment and the type of water treatment depends on the type and intensity of contamination. In fact, the best way or method to avoid contamination of water with heavy metals is to prevent waste water effluent from industries reaching these water bodies. Although, the laws and polices set up by the government and various authorization bodies have roles to play, there is need to have some form of water treatment methodologies to ensure that the water is safe for disposal to the public environment. It is also worthy to note that despite the successes of these methods as various literatures would suggest they also have their specific limitations and disadvantages peculiar to each technique.

2. Experimental

Sample Preparation

The groundnut shells (GS) obtained locally from fruit market Port Harcourt city, Rivers State Nigeria was cut into small particles and then washed with distilled water numerous times to remove impurities, sand and dust. It is then sun dried for two weeks after which it was further shredded by a mill and then sieved using a sieve of 75 μ m.

Preparation of Activated Carbon from groundnut shells using Hydrogen chloride (GS-HCL^C)

150g of the 75µm groundnut shell was chemically modified using acid treatment of 1M Hydrochloric acid as described in a similar process by [3] with some modifications. The acid activation processes were carried out under heating at 60 °C for 2 hours with continuous stirring. The yielded chemically modified material was further chemically activated zinc chloride (ZnCl₂) for (6-8) hours with intermittent stirring at an interval of 2 hours for 30mins to treat the parent adsorbent materials prior to the carbonization process. The produced powder materials after chemical activation were filtered, washed several and then dried at 100 °C for 24 hours. The dried materials were burned for carbonization at a temperature of 400 °C for 2 hours.

Preparation of Activated carbon from Groundnut shells using Potassium Hydroxide (GS-KOH^C)

150g of the groundnut shells with a particle size of 75µm was impregnated in 500 ml of 2wt.% KOH solution for 24 hrs. after which the sample was then filtered and washed with distilled water for several times until the pH is neutral. It was then at dried at 100°C in a Genilab Oven for 12 h before carbonization in Biotech muffle furnace. The temperature for carbonization was set at 400 with a holding time of 2 hrs. the procedure is similar to [4] report with some modifications.

Preparation of functionalized groundnut shells using Tripolyphosphate (GS-TPP)

The procedure used is similar to that as described by [5] with some modifications. A solution of the lignocellulosic biomass was prepared by adding 1L of 2% acetic acid which is 0.1M to a known mass (150g) of the lignocellulose. The solution was then stirred for 30 mins. at an interval of 4hrs for two days. After which a known mass (35.7 gm) of Tripolyphosphate (85% TPP) was then dissolved in 1 litre of double distilled water to prepare 0.1 M solution of TPP. The lignocellulosic particles was then prepared by adding the GS Acetic Acid solution in a drop wise manner to the TPP solution to the ratio 1:1. (GS acetic Acid: TPP v/v). After this, the phosphorylated groundnut shells were then filtered and washed several times with double distilled water.

Proximate Analysis of Groundnut Shell samples

Determination of Cellulose, Lignin and Hemicellulose Content in Groundnut shell was done using Van Soest procedure [6]. The procedure was repeated several times and the average was taken. The pH of the carbon was determined using standard test of ASTM D 3838-80 [7]. Moisture content of activated carbon and raw materials was determined using ASTM D 2867-91 [8]. The volatile content was determined by weighing a known mass of sample and placing it in a partially closed crucible of known weight. It was then heated in a muffle furnace at 900 °C for 3 hrs. The percentage fixed carbon was determined as

$$100 - (\text{Moisture content} + \text{ash content} + \text{volatile matter}). \quad (2.1)$$

Ultimate Analysis

2.00 ± 0.01g of the starch sample was measured into 10ml graduated cylinder and dropped three times on the laboratory table from a height of 2.50 cm to determine the bulk density.

$$B.D = \frac{M(g)}{V_t} \quad \frac{\text{Mass of the starch samples}}{\text{Volume of the packing}}$$

The solution was tested for acidity and or alkalinity at the desired temperature using a HI 2210 Hannah pH meter after which the readings were recorded. The structural and functional modifications of the modified samples were analyzed and compared against the native groundnut shell using FTIR Spectrometer Cary 630. The BET surface area, pore volume and pore size distribution of adsorbents were characterized using Quantachrome Instrument. The elemental composition of the modified and unmodified lignocellulosic samples were analyzed using Scanning Electron Microscope (SEM) Phenom ProX.

Adsorption through Filtration Studies

A standard solution containing containing 1000ppm (1g/l) of the Pb (II) ion metal concentration was prepared by dissolving 1.598g of the Pb(NO₃)₂ salt in double distilled water. Subsequent concentrations were obtained by serial dilution. Effects of each factor were determined keeping other variables constant. All experiments were carried out in triplicates and mean values as well as their standard deviation were calculated using ANOVA. The adsorption capacity that is the metal ions adsorbed onto the resin was calculated using mass balance relation as in equation 2.2 [9].

$$q_e = \frac{(C_o - C_e)V}{M} \quad (2.2)$$

Where: q_e(mg/g) is the adsorption capacity of the adsorbent; C_o and C_e (mg/l) are the initial and final concentration of the metal ions in solution phase, V is the volume of the aqueous solution (l) and M is the weight of the adsorbent (g). The percentage of ions removed was calculated as thus 2.3.

$$\% \text{ of ions Adsorbed} = \frac{(C_o - C_e)}{C_o} \times 100 \quad (2.3)$$

Kinetic Modelling

The kinetics of adsorption process was studied using the non-linear curve fitting method excel solver in Microsoft excel software intra – particle diffusion model and pseudo first and pseudo second order kinetic model. The relationship between the experimental data ($q_{e(\text{exp.})}$) and the model- predicted ($q_{e(\text{calc.})}$) values was expressed by the statistical error analysis tools listed using non-linear excel solver add-in tool in Microsoft excel.

Intra –Particle Diffusion Model

For a batch adsorption process (as used in this study), initial adsorption occurs on the surface of the adsorbent. Also, there is possibility of the adsorbate to diffuse into the interior pores of the adsorbent [10]. Weber and Morris suggested a model to investigate whether the adsorption is intra-particle or not. [11]. The model equation is expressed as;

$$q_t = k_d t^{\frac{1}{2}} + C \quad (2.4)$$

A plot of q_t versus $t^{\frac{1}{2}}$ will give the slope k_d ($\text{mgg}^{-1}\text{min}^{1/2}$) which is the intra-particle diffusion constant and intercept C which is an indication of the boundary layer thickness.

Pseudo First –Order Kinetic Model

Non-linear form used in excel solver model [12]

$$q_t = q_e - \exp(-k_1(q_e - q_t)t) \quad (2.5)$$

Where: k_1 (min^{-1}) is the rate constant of the Pseudo first-order sorption, q_t (mg/g) denote the amount of sorption at time t (min), q_e (mg/g) is the amount of sorption at equilibrium.

Pseudo Second –Order Kinetic Model

In non-linear is given as [12].

$$q_t = \frac{q_e^2 k_2 t}{q_e k_2 t + 1} \quad (2.6)$$

Where $v_o = K_2 q_e^2$ (mg/g-min) is the initial sorption rate, K_2 ($\text{g mg}^{-1}\text{min}^{-1}$) correspond to the rate constant of sorption, q_e (mg/g) is the amount of metal ion adsorbed at equilibrium and q_t (mg/g) is the amount of metal ion on the surface of the sorbent at any time t (min). The pseudo-second order kinetic model describes the rate-limiting step as chemisorption involving exchange of electrons between the adsorbate and the adsorbent [12].

Thermodynamics of Adsorption

Thermodynamic parameters ΔH , ΔS , and ΔG are calculated using equation 2.7

$$\ln \frac{Q}{C_e} = \frac{-\Delta H}{RT} + \frac{\Delta S}{R} \quad (2.7)$$

R is the Gas law constant = $8.314\text{J (mol K)}^{-1}$, T is the temperature in Kelvin (K) ΔH and ΔS are determined from the slope and intercept respectively of the linear plot of $\frac{Q}{C_e}$ versus $\frac{1}{T}$ [13]. Gibbs free energy of adsorption ΔG (kJ/mol) is calculated from the values of ΔH and ΔS using equation 2.8

$$\Delta G = \Delta H - T\Delta S \quad (2.8)$$

Error Analysis

The traditional methods of determining the isotherm parameters by linear regression appear to give a good fit to experimental data. However, the R_2 (Spearman correlation coefficient or coefficient of determination) is based on the linear forms of the isotherm equations and does not represent the errors in the isotherm curves. To evaluate the fit of the isotherm equations to the experimental data, different error functions of non-linear regression were used here to determine the constants model parameters for the non-linearized data fitting. The Sum square of Errors (ERRSQ), residual root mean square error (RMSE) and chi-square test (X^2) were used.

The Sum Square of Errors (ERRSQ)

The sum of square of errors (ERRSQ) is a broadly used error function. This method can be represented by the following expression [14]:

$$\sum_{i=1}^n (q_{e(\text{calc.})} - q_{e(\text{exp.})})^2 \quad (2.9)$$

where $q_{e(\text{calc.})}$ is the theoretical concentration of adsorbate on the adsorbent, which is calculated from the isotherm models. $q_{e(\text{exp.})}$ is the experimentally measured adsorbed solid phase concentration of the adsorbate adsorbed on the adsorbent. A major disadvantage of this error function is that at higher end of liquid-phase adsorbate concentration ranges the isotherm parameters derived using this error function will provide a better fit as the magnitude of the errors and therefore the square of errors tend to increase illustrating a better fit for experimental data obtained at the high end of concentration range.

Root Mean Square Error Test (RMSE)

RMSE can be defined [12]

$$\sqrt{\frac{1}{n-2} \sum_{i=1}^n (q_{e(\text{exp.})} - q_{e(\text{calc.})})^2} \quad (2.10)$$

The subscripts “exp” and “cal” show the experimental and calculated values and n is the number of observations in the experimental isotherm. The smaller the RMSE value, the better the curve fitting.

Nonlinear Chi-Square Test (χ^2)

This function is important in the determination of the best fit of an adsorption system. It can be obtained by judging the sum of squares difference between experimental and calculated data, with each square difference divided by its corresponding values. If the data from the model calculation are close to the experimental data, χ^2 will be a small number; [12] the χ^2 value can be used to measure how well the model fits. The value of this function can be obtained from the following equation:

$$\sum_{i=1}^n \frac{(q_{e(\text{calc.})} - q_{e(\text{exp.})})^2}{q_{e(\text{exp.})}} \quad (2.11)$$

3. RESULTS AND DISCUSSION**Table -3.1 Proximate Analysis of Samples**

Properties	GS	GS-HCL ^C	GS-KOH ^C	GS-TPP
Cellulose Content	46.6333 ^{0.8002}	N/A	N/A	N/A
Lignin Content	21.8 ^{1.2489}	N/A	N/A	N/A
Hemicellulose Content	17.2 ^{1.7000}	N/A	N/A	N/A
Moisture Content	9.8091 ^{0.4340}	10.1556 ^{0.4873}	10.6303 ^{1.3062}	9.2362 ^{0.6673}
Ash Content	22.6135 ^{0.2844}	1.8894 ^{0.3363}	7.5763 ^{1.4516}	35.6003 ^{0.5595}
Volatile Matter	62.67303 ^{0.8287}	18.1306 ^{0.9518}	9.6004 ^{0.1798}	40.8358 ^{1.2963}
Fixed Carbon Content	4.9046 ^{0.2450}	69.8278 ^{0.5220}	71.6214 ^{0.6230}	14.3277 ^{1.2417}

Experiments were carried out in triplicates

Results displayed are mean and standard deviation (mean^{standard deviation})

N/A means not applicable

The groundnut shells after being washed, dried and ground were analyzed to determine their proximate content as displayed in Table 4.2. The results of the cellulose, hemicellulose and lignin content were 46.6333%, 21.8% and 17.2% respectively. The results are comparable with [15]. The moisture content of the groundnut shells did not vary much after modification of the various samples. Carbonization was observed to increase the carbon content of the samples of GS-HCL^C and GS-TPP^C while decreasing the volatile matter as compared to the native Groundnut shells GS a similar observation was in the work of [16] Benzaghi Li. and Malik et al [17]. Upon activation and exposure to high temperatures (400°C) the groundnut shells show a considerable decrease in volatile matter content a similar observation was also noticed although to a lesser degree during the analysis of treatment of GS with Tripolyphosphate leading the adsorbent GS-TPP.

Result of Ultimate Analysis**Table -3.2 pH and Bulk Density Result of Samples**

Properties	GS	GS-HCL ^C	GS-KOH ^C	GS-TPP
pH	5.9	4.7	9.9	8.7
Bulk Density	0.2667 ^{0.0000}	0.2469 ^{0.0000}	0.2778 ^{0.0000}	0.3333 ^{0.0000}

Experiments were carried out in triplicates

Results displayed are mean and standard deviation (mean^{standard deviation})

N/A means not applicable

The pH of the samples was analyzed and results indicated the table above the pH observed is in direct relationship to the type of chemicals used for activation and functionalization of the adsorbents. The bulk density is inversely proportional to particle size. It therefore suggests that as bulk density decreases, particle size is meant to increase. There was an increase in bulk density of the GS-KOH^C and GS-TPP Samples which depicts decrease in particle sizes while for the GS-HCL^C sample there was a slight decrease.

FTIR Spectra

The results of the FTIR spectra of the unmodified, modified and functionalized ground nut shell GS, GS-HCL^C, GS-KOH^C and GS-TPP are shown in figures 3.1, 3.2, 3.3 and 3.4 respectively.

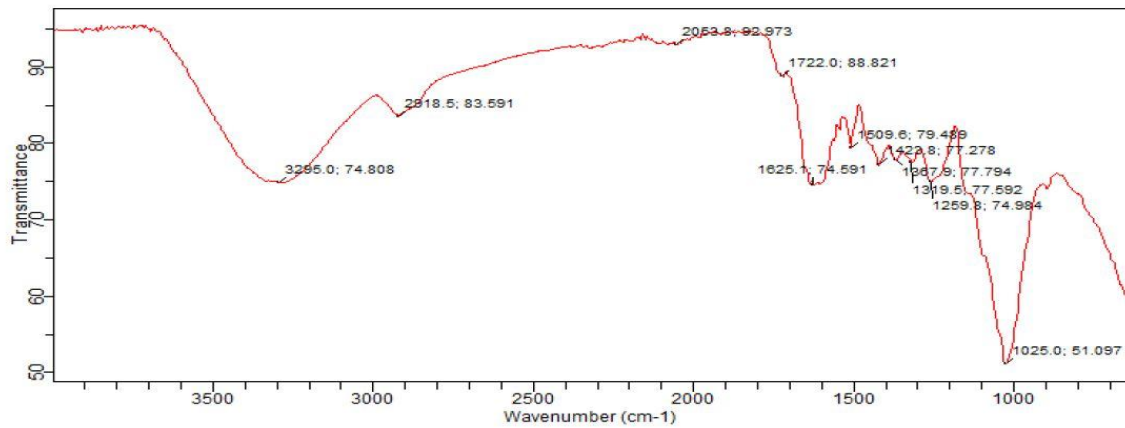


Fig. 3.1 FTIR Spectra of GS

The FTIR Spectra of the unmodified groundnut shell is similar to that of Sunil Kumar et al [18]. Comparing both reports shows the presence of -OH stretching groups at 3295cm^{-1} and 3398cm^{-1} , alkane stretching at 2918cm^{-1} and 2929cm^{-1} , C=C stretching at 1625cm^{-1} and 1600cm^{-1} and -CH₃ bending vibration at 1367cm^{-1} and 1363cm^{-1} for the GS and Sunil Kumar et al FTIR spectra's respectively. The Spectra also correlates with [19] groundnut shell FTIR spectra.

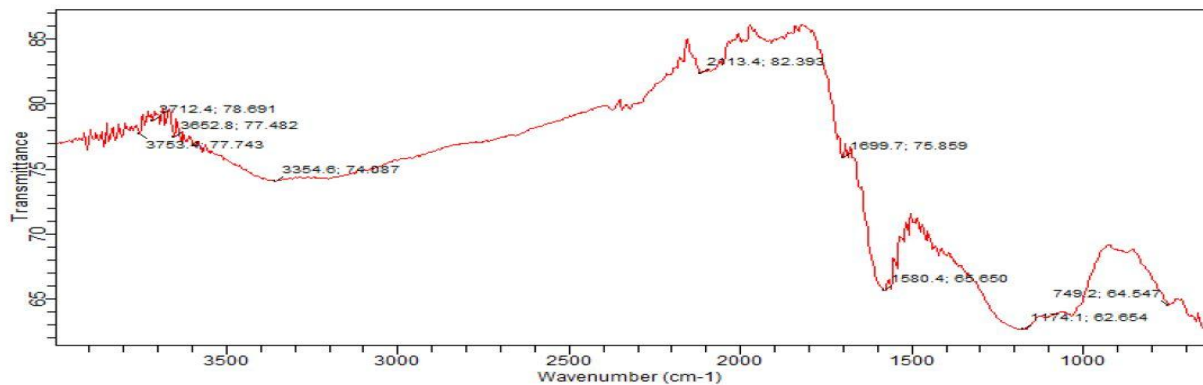


Fig. 3.2 FTIR Spectra of GS-HCL^C

The spectra of the activated and carbonized NLC using Hydrochloric acid and Zinc chloride GS-HCL^C spectra is in Figure 4.2 above. Some distinctive peak bands are present in the spectra such as the rough peaks at 3753cm^{-1} , 3712cm^{-1} and 3652cm^{-1} respectively and they are indicative of -OH stretching [20]. The broad band peak at 3354cm^{-1} is definitive of -OH stretching functional groups. This broadband also appeared in the unmodified groundnut shell GS and the other modified samples. There were also noticeably medium weak multiple bands at 1580cm^{-1} suggesting the presence of C=C aromatic stretching. Also, the well-defined broad band peak at 1174cm^{-1} suggests the presence of C-O functional groups. The peak at 749.2 is indicative of aliphatic Chloro-carbon C-Cl bonding [21].

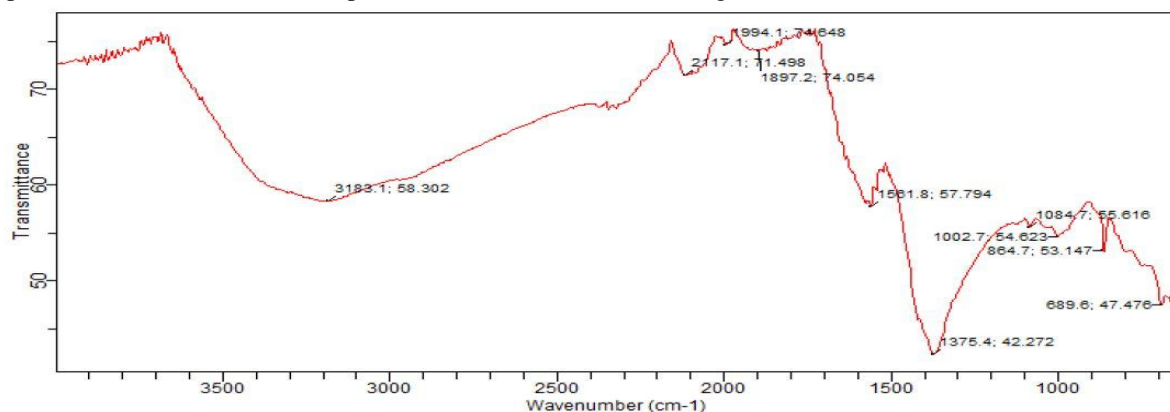


Fig. 3.3 FTIR Spectra of GS-KOH^C

The FTIR spectra of GS-KOH^C shows a distinctive peak at 3183cm^{-1} . This peak describes an alcohol or OH groups which has a very distinct broad shape around 3650cm^{-1} - 3200cm^{-1} . Other peaks of notable importance here are the peaks between 1200 - 1050 denoting presence of primary, secondary and tertiary alcohols that is C - O bonds approximately at 1050 , 1100 and 1150 respectively [21]. The sharp peak at 1375cm^{-1} is indicative of the presence of a methyl group with either a symmetric or asymmetric bend.

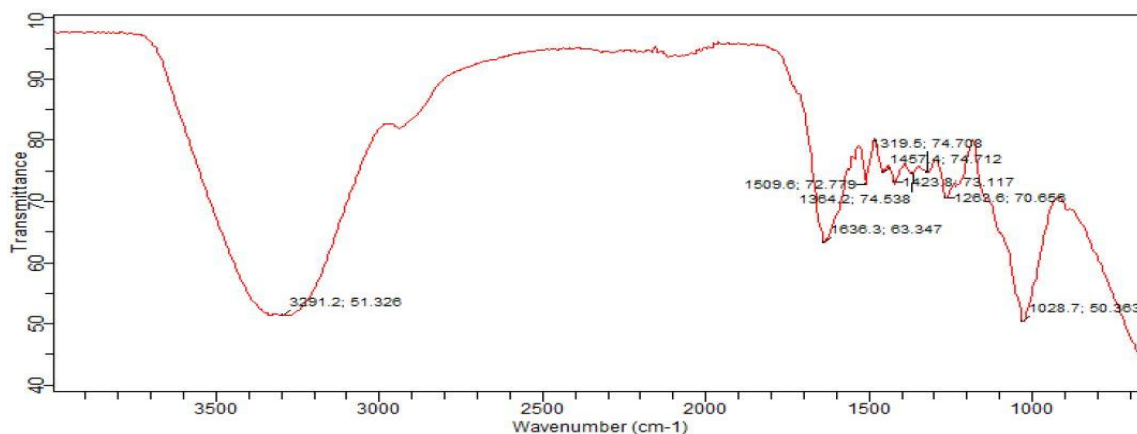


Fig. 3.4 FTIR Spectra of GS-TPP

The FTIR spectra of GS-TPP shows a very glaring peak at 3291cm⁻¹this peaks describes an alcohol or OH groups which has a very distinct broad shape around 3650cm⁻¹ - 3200cm⁻¹. The sharp peak at 1028.7cm⁻¹ describes the presence of a phosphate ion. The range of multiple peaks from 1509cm⁻¹ – 1262cm⁻¹ indicates presence of organophorous compound and phosphorous oxide functional groups as described by Infrared Spectroscopy correlation table. [20]. The spectra between 1500 cm⁻¹ - 900 cm⁻¹ is highly similar to that of the spectra of TPP as described by National Institute of standards and Technology [22]. This shows that indeed the functionalization of Groundnut shells with Tripolyphosphate occurred as described by the presence of the functional groups in the spectra.

Surface Area Analysis

Table -3.3 Surface Area Analysis of Adsorbents

Adsorbents	specific surface area SBJH, (m ² /g)	Pore Volume (V) (cm ³ /g)	Average Pore Diameter or size (R) (nm)
GS-HCL ^C	957.0	0.4614	2.093
GS-KOH ^C	412.5	0.2031	2.138
GS-TPP	397.9	0.1958	2.447

BJH is a method to determine pore size distribution of a mesoporous solid based on the Kelvin equation. The results show that all the adsorbents are mesoporous materials since their pore diameter is between 2 and 50nm according to IUPAC [20] and have porosities on a nano scale. The average pore diameter is observed to increase as follows GS-TPP > GS-KOH^C > GS-HCL^C. Generally, as in the case of adsorption, larger surface area increases the extent of adsorption and surface reactivity of the adsorbents hence, as expected and described in the adsorption studies GS-HCL^C with surface area of 957.0m²/g which has the largest surface area and an excellent adsorption capability while GS-TPP has the least adsorption performance with surface area at 397.9m²/g. The surface area increases in the order of GS-HCL^C > GS-KOH^C > GS-TPP. Also surface area is a direct indication of particle size therefore, greater the surface area, the smaller the particle size [23]. Hence the particle size decreases in order of GS-HCL^C < GS-KOH^C < GS-TPP. This is also confirmed in the analysis of the SEM Micrographs. Analysis of the BJH pore volume through the plot of the pore size distribution shows the pore volume increases on the order of GS-HCL^C > GS-KOH^C > GS-TPP. The pore volume advocates an indication of the total pore volume in one gram of the adsorbent.

Lead Adsorption Kinetic Studies

Lead Adsorption Kinetic Modelling on GS-HCL^C Adsorbent

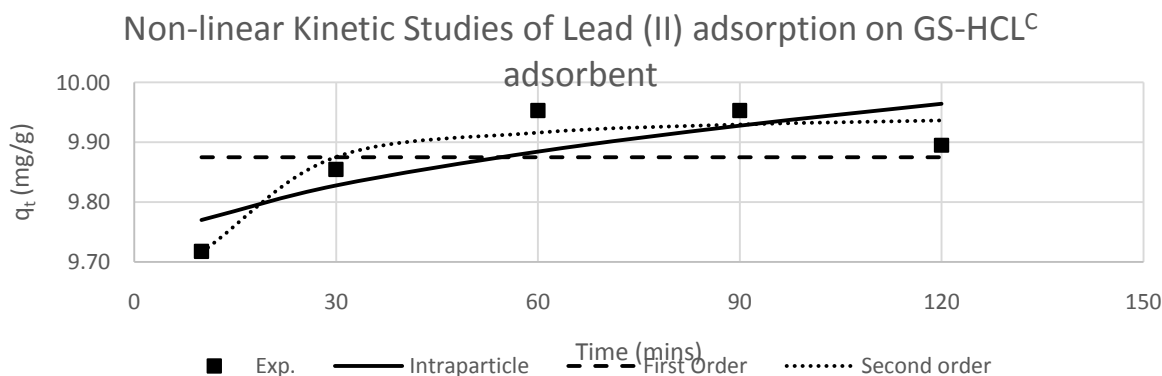


Fig. 3.5 Adsorption Kinetic graphical modelling for lead adsorption on GS-HCL^C

Table -3.4 Classical Isotherm model parameters for GS-HCL^C lead (II) ion adsorption

GS-HCL ^C	Intraparticle	Pseudo First order	Pseudo Second Order
q_e		9.8747	9.9570
K	0.0250	4.0200	0.4049
C	9.6909		
ERRSQ	0.0136	0.0378	0.0041
RMSE	0.0674	0.1122	0.0368
χ²	0.0003	0.0008	0.0001

The values in table 3.4 above indicates the presence of boundary layer effect ($K > 0$). It is worthy to note that the q_e exp. values q_e calc. values for this model were close and hence can describes the kinetics of adsorption. However, it also shows that intra-particle diffusion model is not the only rate controlling step since the line did not pass the origin and hence other kinetic models were investigated. The results of Pseudo first kinetic model and pseudo second order kinetic models from table and table show that both models can explain the kinetics of sorption. In both models the q_e calc. values were a close fit to q_e exp. values and hence the error values were low as described in table 3.4. Pseudo second order kinetic order proved to be a better fit having the lowest errors based on the comparison of error analysis modelling.

Lead Adsorption Kinetic Modelling on GS-KOH^C Adsorbent

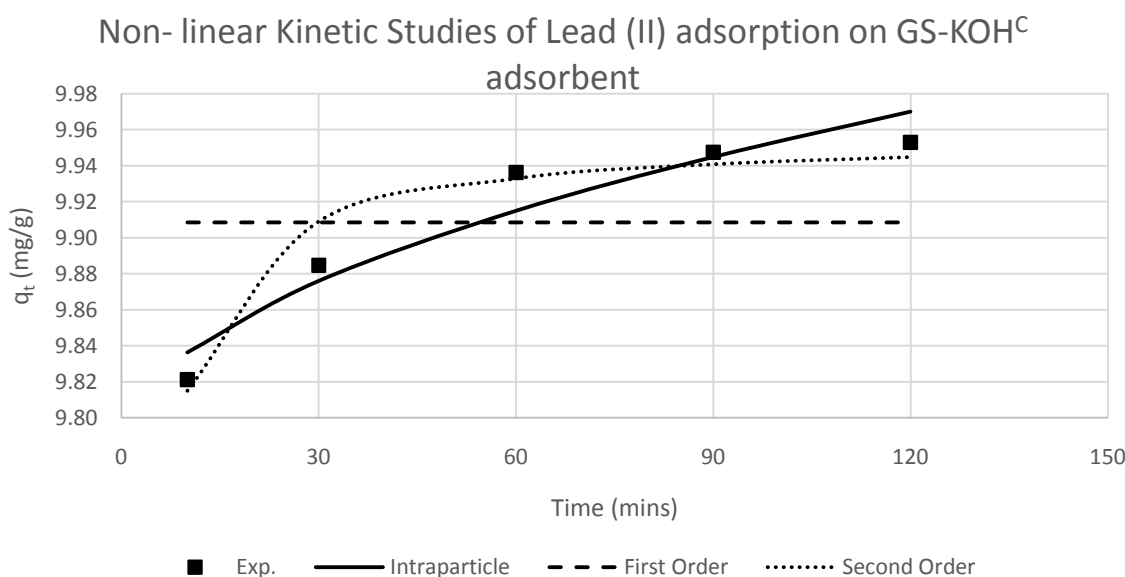


Fig. 3.6 Adsorption Kinetic graphical modelling for lead adsorption on GS-KOH^C

Table -3.5 Classical Isotherm model parameters for GS-KOH^C lead (II) ion adsorption

GS-KOH ^C	Intraparticle	First order	Second Order
q_e		9.9085	9.9568
K	0.0172	4.3997	0.6950
C	9.7821		
ERRSQ	0.0011	0.0125	0.0008
RMSE	0.0187	0.0644	0.0159
χ²	0.0000	0.0003	0.0000

In the modelling of GS-KOH^C the presence of boundary layer effect ($K = 0.0172$) was observed and also the intraparticle diffusion model was not the only rate limiting step since intercept ($C = 9.7821$) did not pass the origin. All three models can describe the kinetics of sorption however Pseudo second order kinetic model based on error analysis best describes rate of adsorption of lead on the GS-KOH^C adsorbent with q_e at 9.9568mg/g.

Lead Adsorption Kinetic Modelling on GS-TPP Adsorbent

It is important to note that the results of kinetic studies for the graph shows that desorption of the lead metal ions increases with increase in agitation time. The negative value of K indicates the absence boundary layer effect also the Intercept C did not pass through the origin. These factors indicate that Intraparticle diffusion model cannot be used to describe the rate of kinetics and therefore is not the only rate controlling step of the adsorption process. The low values of ERRSQ, RMSE and χ^2 indicate that Pseudo first kinetic model and Pseudo second order Kinetic model can be used to

describe the rate of adsorption kinetics. Intra-particle diffusion model based on the plot and error analysis best describes the kinetics of sorption of lead (II) ions on the GS-TPP adsorbent.

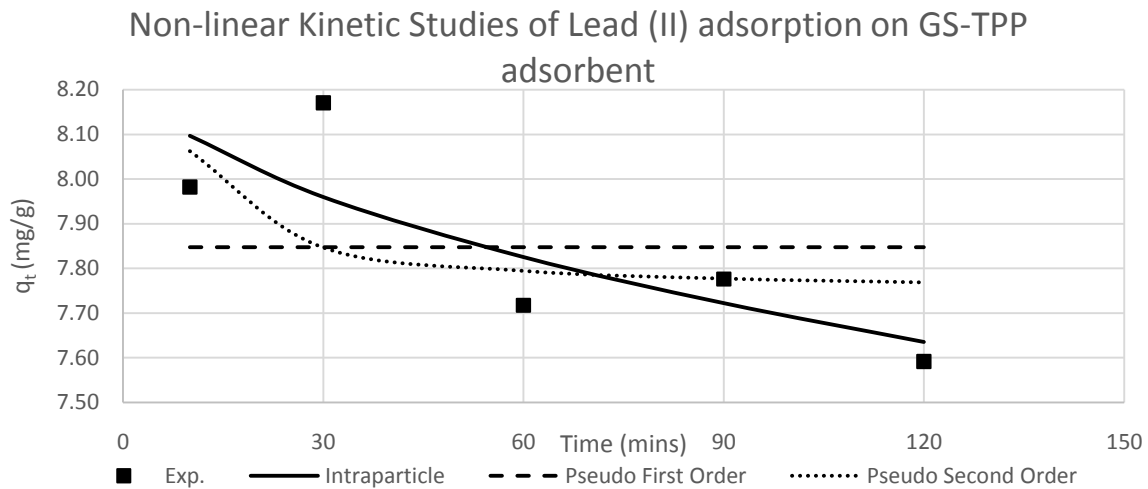


Fig. 3.6 Adsorption Kinetic graphical modelling for lead adsorption on GS-TPP
 Table -3.6 Classical Isotherm model parameters for GS-TPP lead (II) ion adsorption

GS-TPP	Intraparticle	First order	Second Order
q_e		7.8478	7.7428
K	-0.0592	2.2617	-0.3259
C	8.2839		
$ERRSQ$	0.0740	0.2099	0.1485
$RMSE$	0.1571	0.2645	0.2225
χ^2	0.0019	0.0053	0.0038

Adsorption Thermodynamics

The thermodynamic parameters provide useful information on the energetic changes of the adsorption process. The parameters were derived through a plot of $\ln q_e/C_e$ against $1/T$ as shown in figure 3.7. below. The thermodynamic parameters ΔH , ΔS and ΔG are in table 3.7 below.

Table -3.7 Table of Plot of $\ln(q_e/C_e)$ versus $1/T$

Plot of $\ln(q_e/C_e)$ versus $1/T$ for the adsorption of Pb(II) ions onto adsorbents										
T (°K)	1/T (°K)	GS-HCL ^c			GS-KOH ^c			GS-TPP		
		C_e	q_e	$\ln(q_e/C_e)$	C_e	q_e	$\ln(q_e/C_e)$	C_e	q_e	$\ln(q_e/C_e)$
293	0.003413	1.2147	9.7571	2.0835	0.9586	9.8083	2.3255	30.9600	3.8080	-2.0956
303	0.003300	0.2597	9.9481	3.6456	0.2283	9.9543	3.7751	9.3740	8.1252	-0.1430
313	0.003195	0.3390	9.9322	3.3775	0.2660	9.9468	3.6215	8.9686	8.2063	-0.0888
323	0.003096	0.5773	9.8845	2.8403	0.4170	9.9166	3.1689	11.2460	7.7508	-0.3722
333	0.003003	0.7206	9.8559	2.6157	0.6047	9.8791	2.7934	14.5917	7.0816	-0.7229

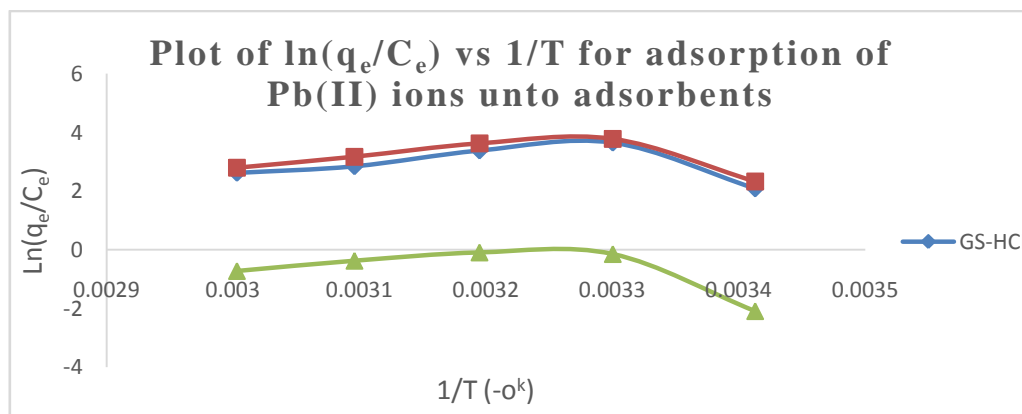


Fig. 3.7 Plot of $\ln(q_e/C_e)$ vs $1/T$ for the adsorption of Pb (II) ions onto adsorbents

Table -3.8

Adsorbents	T (°C)	Pb ²⁺		
		ΔH (kJ/mol)	ΔS (kJmol ⁻¹ K ⁻¹)	ΔG (kJ/mol)
GS-HCL ^C	20	3.11874768	0.034199639	-6.901746547
	30			-7.243742937
	40			-7.585739327
	50			-7.927735717
	60			-8.269732107
GS-KOH ^C	20	3.71228414	0.03796505	-7.411475393
	30			-7.791125889
	40			-8.170776385
	50			-8.550426881
	60			-8.930077377
GS-TPP	20	21.6928888	0.063758403	3.011676662
	30			2.37409263
	40			1.736508598
	50			1.098924566
	60			0.461340534

The table 3.8 above shows the inherent energy change of sorption for the adsorption of Pb (II) ions and Ni (II) by all three adsorbents GS-HCL^C, GS-KOH^C and GS-TPP. Enthalpy change ΔH is positive for all three adsorbents. Since the heat of sorption is low (<40kJ/mol) it is assumed that the adsorption process is physical or physisorption. The positive values of ΔS during the adsorption of both lead of all three adsorbents also indicate increase in degree of randomness at the adsorbent – adsorbate interface during adsorption. The negative value of free energy ΔG was observed in all adsorption processes except the adsorption of lead ions by GS-TPP for change indicate that the adsorption is spontaneous and hence the reaction is exergonic. It therefore means that no external energy is required for the reaction process to take place. Positive values of ΔG was however observed during the adsorption of lead ions by GS-TPP indicating that in this adsorption process the reaction was not spontaneous.

4. CONCLUSION

The physico-chemical and adsorptive properties of groundnut shell based adsorbent also indicate its excellent potential for use as an adsorbent for applicability in water and wastewater treatment system since the adsorbents showed high efficiencies with only 0.25g of each adsorbent. Pseudo second kinetic order best describe the adsorption of lead on the carbonized adsorbents while Intraparticle diffusion best describes the rate of adsorption for the GS-TPP adsorbent. From the experimental analysis and results obtained. The enthalpy changes were all positive for all three adsorbents and Gibb's free energy was negative except when the GS-TPP adsorbent was used indicating the adsorption process was endothermic and spontaneous in nature respectively except during the adsorption of Ni²⁺ by GS-TPP where the reaction process was not spontaneous.

REFERENCES

- [1]. Singh Mann, U., Dhingra, A., & Singh, J. (2014). Water Pollution: Causes, Effects and Remedies. *International Journal of Advanced Technology in Engineering and Science* *Www.ijates.com*, 2(2), 2348–7550.
- [2]. Adelekan, B. A., & Abegunde, K. D. (2011). Heavy metals contamination of soil and groundwater at automobile mechanic villages in Ibadan, Nigeria. *International Journal of the Physical Sciences*, 6(5), 1045–1058. <http://doi.org/10.5897/IJPS10.495>
- [3]. Elkady, M. F., Hussein, M. M., & Atiaa, H. M. (2015). Preparation of nano-activated carbon from carbon based material for copper decontamination from wastewater. *American Journal of Applied Chemistry*, 3, 31–37. <http://doi.org/10.11648/j.ajac.s.2015030301.15>
- [4]. Pagketanang, T., Artnaseaw, A., Wongwicha, P., & Thabuot, M. (2015). Microporous Activated Carbon from KOH-Activation of Rubber Seed-Shells for Application in Capacitor Electrode. *Energy Procedia* (Vol. 79). Thailand: Elsevier Ltd. <http://doi.org/10.1016/j.egypro.2015.11.5>
- [5]. Maram T. H. Abou Kana, Mohammed Radi, & Maher Z Elsabee. (2013). Wastewater Treatment With Chitosan Nano-Particles *International Journal of Nanotechnology and Application* (IJNA) ISSN 2277-4777 Vol. 3, Issue 2, Jun 2013, 39-50 © TJPRC Pvt. Ltd
- [6]. Van Soest, P.J., J.B. Robertson & B.A. Lewis, 1991. Methods for dietary fiber, neutral detergent fiber and nonstarch polysaccharides in relation to animal nutrition. *J. Dairy Sci.*, 74, 3583-3597
- [7]. American Society for Testing and Materials: Standard Method for the Determination of pH value in Biomass ASTM D 3838-80, Philadelphia, P.A.: 11, (05), 1996.
- [8]. American Society for Testing and Materials: Standard for Method for Moisture in Activated Carbon ASTM D 2867-91, Philadelphia, PA: ASTM Committee on Standards, 1991

- [9]. Ahmad, M. A., Herawan, S. G., & Yusof, A. A. (2014). Equilibrium, Kinetics, and Thermodynamics of Remazol Brilliant Blue R Dye Adsorption onto Activated Carbon Prepared from Pinang Frond. *ISRN Mechanical Engineering*, 2014, 1–7. <http://doi.org/http://dx.doi.org/10.1155/2014/184265>
- [10]. Sivakumar, P., & Palanisamy, P. N. (2009). Adsorption studies of basic Red 29 by a non-conventional activated carbon prepared from Euphorbia antiquorum L. *International Journal of Chem. Tec. Research*, 1 (3), 502-510.
- [11]. Oladoja N.A, & Asia I.O. (2008). Studies on the sorption of basic dye by rubber (Heveabrasiliensis) seed Shell, *Turkish J. Eng. Env. Sci.*, 32, 2008, 143-152
- [12]. Samarghandi, M. R., Hadi, M., Moayedi, S., & Askari, F. B. (2009). Two-Parameter Isotherms of Methyl Orange Sorption by Pinecone Derived Activated Carbon. *Iran Journal of Environmental Health Science and Engineering*, 6(4), 285–294.
- [13]. Thilagan, J., Gopalakrishnan, P. S., & Kannadasan, T. (2013). Thermodynamic study on adsorption of Copper (II) ions in aqueous solution by Chitosan blended with Cellulose & cross linked by Formaldehyde, Chitosan immobilised on Red Soil, Chitosan reinforced by Banana stem fibre. *International Journal of Scientific Research Engineering & Technology (IJSRET)*, 2(April), 28–36.
- [14]. Ayawei, N., Ebelegi, A. N., & Wankasi, D. (2017). Modelling and Interpretation of Adsorption Isotherms. *Journal of Chemistry*, 2017, 1–11. Retrieved from <https://doi.org/10.1155/2017/3039817>
- [15]. Bharthare, P., Preeti, S., Singh, P., & Archana, T. (2014). Peanut Shell as Renewable Energy Source and Their Utility in Production of Ethanol. *International Journal of Advance Research*, 2(4), 1–12.
- [16]. Li, Benghazi. (2011). Characterization of Pore Structure and Surface Chemistry of Activated Carbons – A Review.
- [17]. Malik, R., Ramteke, D. S., & Wate, S. R. (2006). Physico-chemical and surface characterization of adsorbent prepared from groundnut shell by ZnCl₂ activation and its ability to adsorb colour, *13(July)*, 319–328.
- [18]. Sunil Kumar, Gunasekar, V., & Ponnusami, V. (2013). Removal of Methylene Blue from Aqueous Effluent Using Fixed Bed of Groundnut Shell Powder. *Journal of Chemistry*, 2013, 1–5. <http://doi.org/10.1155/2013/259819>
- [19]. Prithivirajan, R., Jayabal, S., Sundaram, S. K., & Sangeetha, V. (2015). Hybrid biocomposites from agricultural residues: mechanical, water absorption and tribological behaviors. *Journal of Polymer Engineering*, 1–9. <http://doi.org/10.1515/polyeng-2015-0113>
- [20]. Wikipedia. (2017, March 24). <https://en.wikipedia.org/wiki/Adsorption#BET>. Retrieved from From Wikipedia, the free encyclopedia: <https://en.wikipedia.org/wiki/Adsorption#BET>
- [21]. Coates, J. (2000). Interpretation of Infrared Spectra, A Practical Approach. In *Encyclopedia of Analytical Chemistry* (R.A. Meyer, pp. 10815–10837). John Wiley & Sons Ltd, Chichester. <http://doi.org/10.1002/9780470027318.a5606>
- [22]. Coblenz (2017). National institute of Science and Technology NIST. NIST chemistrywebBook. <https://webbook.nist.gov/chemistry>
- [23]. Valenzuela-Muñiz, A. M. (2012). *Surface Area and Pore Size Distribution* (ABC's of Electrochemistry series Materials Characterization techniques). *Surface Area and Pore Size Distribution*. Ohio.